Progress in Nuclear Energy 109 (2018) 250–263

Contents lists available at ScienceDirect

Progress in Nuclear Energy

journal homepage: www.elsevier.com/locate/pnucene

Flow structures associated with CSRDM shroud tube and control rod assembly: A combined experimental and simulation study

Ankit Kumar Gautam[a], Pradipta Kumar Panigrahi[a,*], Karuppanna Velusamy[b]

[a] Department of Mechanical Engineering, Indian Institute of Technology Kanpur, Kanpur, 208016, India
[b] Nuclear Systems Analysis Group, Indira Gandhi Centre for Atomic Research, Kalpakkam, 603102, India

ARTICLE INFO

Keywords:
FBR
Porous tube
CFD
Power law exponent
Liquid-gas interface
Jet impingement

ABSTRACT

This paper presents numerical investigation of flow behavior near a submerged porous shroud tube, a protective covering over Control Safety Rod Driving Mechanism (CSRDM) inside liquid sodium coolant pool of a Fast Breeder Reactor (FBR) in synergy with corresponding experimental findings to explicate possible gas entrainment mechanism inside the liquid pool. Fluid entering the shroud tube whose top end is just below the free surface causes swelling of free surface near the axial outlet of the shroud tube that vastly affects the flow behavior nearby and liquid-fall type gas entrainment inside the coolant pool. To numerically capture the effects of various flow rate and free surface height on the flow behavior near the shroud tube, an approximate single phase realizable $k-\varepsilon$ turbulence flow model has been implemented. The study is performed assuming Froude number similarity for Reynolds number ranging from 1.3×10^3 to 6.5×10^3 and corresponding Froude number ranging from 0.266 to 1.332. Both computational and experimental studies have been carried out with water as the working fluid. Geometry of hump profile, obtained experimentally, has been incorporated as input to the computation to avoid large computational time associated with free surface modeling. With such a coupled approach, a strong agreement is obtained between numerical prediction and experimental Schlieren and dye visualization results. The simulation study is subsequently used to report the radial and axial velocity and turbulence intensity distribution in the liquid pool. The nature of impinging jet-like velocity profile from the axial exit of the shroud tube and corresponding boundary layer-like growth near the air-water interface is compared with that of the free wall jet, impinging wall jet and impinging confined wall jet. The free surface boundary layer growth follows power law similar to that of the wall jet in low Froude number regime ($Fr < 0.666$). At higher Froude number, the axial flow along the shroud tube dominates over the radial free surface flow. The power law exponent of the free surface boundary layer growth is lower compared to that of the wall jet due to the lower viscous effect from the adjacent air medium and axial flow due to the hump entrainment.

1. Introduction

In sodium cooled fast breeder reactors, the core is submerged in a large liquid sodium pool and the Control Safety Rod Drive Mechanisms (CSRDMs) which are sub-components of Control Plug (CP) assembly, are located just above the reactor core. As a result of this typical arrangement, the CSRDM assembly is subjected to cross flow and the associated risk of Flow Induced Vibration (FIV). To protect CSRDM against FIV, a porous shroud tube is provided around each CSRDM. Liberal radial gap between the shroud tube and CSRDM helps in easy introduction or withdrawal of CSRDM rod during seismic conditions. It also accommodates the thermally induced bowing of control rod subassembly and the associated radial movement of CSRDM with respect to the shroud tube. This liberal gap is the main reason for large flow entry into the control plug assembly. The core outlet flow that enters the annulus of the shroud tube and CSRDM partly discharges into the control plug axially. The axial discharge is responsible for hump formation and gas entrainment at the free surface of the coolant pool. A long shroud tube extending up to the free surface of the sodium pool leads to formation of hump at the free surface and the associated risk of argon gas entrainment into the liquid sodium. A short shroud tube on the other hand would not serve the purpose of protecting the CSRDM against FIV. Hence, the radial gap between the CSRDM and the shroud tube, and the submergence depth of the shroud tube have to be optimized.

The liquid sodium coolant exits the reactor core at a temperature of

* Corresponding author.
E-mail address: panig@iitk.ac.in (P.K. Panigrahi).

https://doi.org/10.1016/j.pnucene.2018.08.016
Received 26 May 2018; Received in revised form 1 August 2018; Accepted 27 August 2018
Available online 02 September 2018
0149-1970/

Table 1
Details of perforation arrangement of the prototype (Natesan et al. (6)) and 1/9 scale model of the shroud tube.

	n	d (mm)	d/D	$N \times M$	P_c (mm)	P_v (mm)	P_c/D	P_v/D	ϕ (%)
Prototype	90	60	0.279	15 × 6	112.57	189.28	0.5236	0.8804	12.991
Model	90	6.4	0.266	15 × 6	12.56	21.13	0.5236	0.8804	11.862

n: Perforation count, d: Perforation diameter, D: Shroud tube inner diameter, N: Number of rows, M: Number of perforations in a row, P_c: Circular pitch corresponding to inner diameter of shroud tube, P_v: Vertical pitch and ϕ: Porosity of shroud tube.

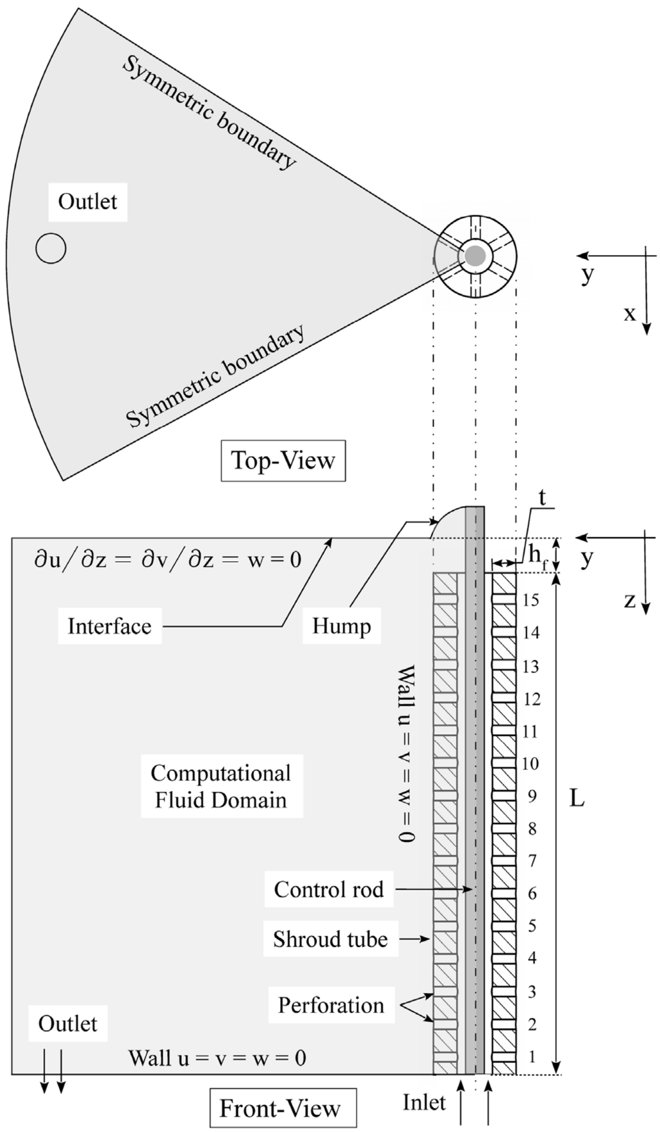

Fig. 1. Schematic representing the top and front view 60° sector of axi–symmetric computational fluid domain marked with respective boundary conditions. Perforation row number, 1 to 15, has been marked alongside the shroud tube.

~547 °C and about 15% (Gautam et al. (2017)) of total amount of coolant enters through the annular gaps of assembly placed just above the reactor core. The perforations of the shroud tube serves two important purposes: (a) it reduces the axial flow velocity by partial diversion of flow in radial direction and (b) it mitigates axial temperature stratification inside the CP shell due to redistribution of the flow around the shroud tube. Nonetheless, a substantial amount of flow exits from the axial outlet submerged below the free surface. This leads to high free surface velocity and swelling of free surface causing entrainment of gas bubbles inside the coolant pool. Entrained gas bubbles lead to

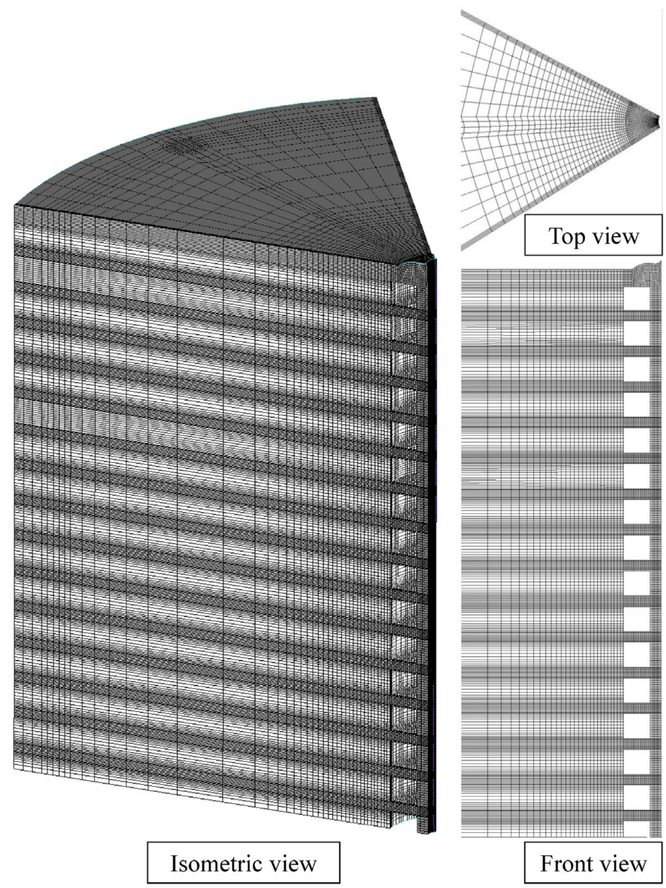

Fig. 2. Sample mesh grids for 60°sector of the computational domain in full isometric view along with the zoomed front view and top view.

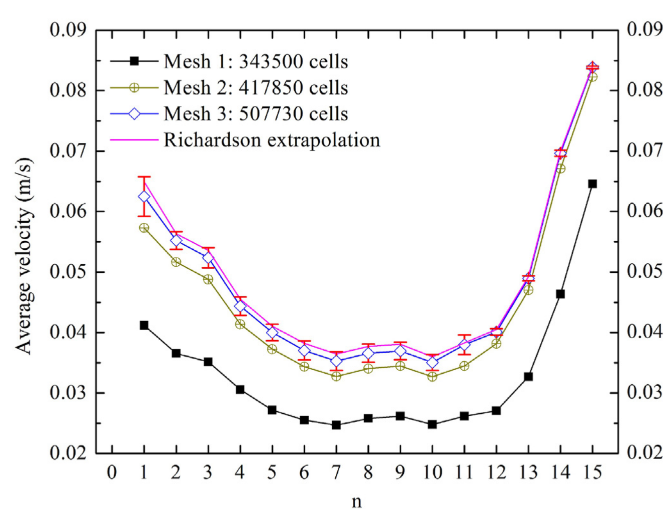

Fig. 3. Variation of average velocity at the exit of different perforation rows (See Fig. 1) using different type of mesh for Froude number, $Fr = 0.266$, and free surface height, $h_f/L = 0.031$.